

CoSSegGaussians: Compact and Swift Scene Segmenting 3D Gaussians with Dual Feature Fusion

Bin Dou¹, Tianyu Zhang¹, Yongjia Ma¹, Zhaohui Wang¹, Zejian Yuan^{1*}

¹Institute of Artificial Intelligence and Robotics, Xi'an Jiaotong University
 {abc991227db, puzzling229, maguire, astjk112345}@stu.xjtu.edu.cn, yuan.ze.jian@xjtu.edu.cn,

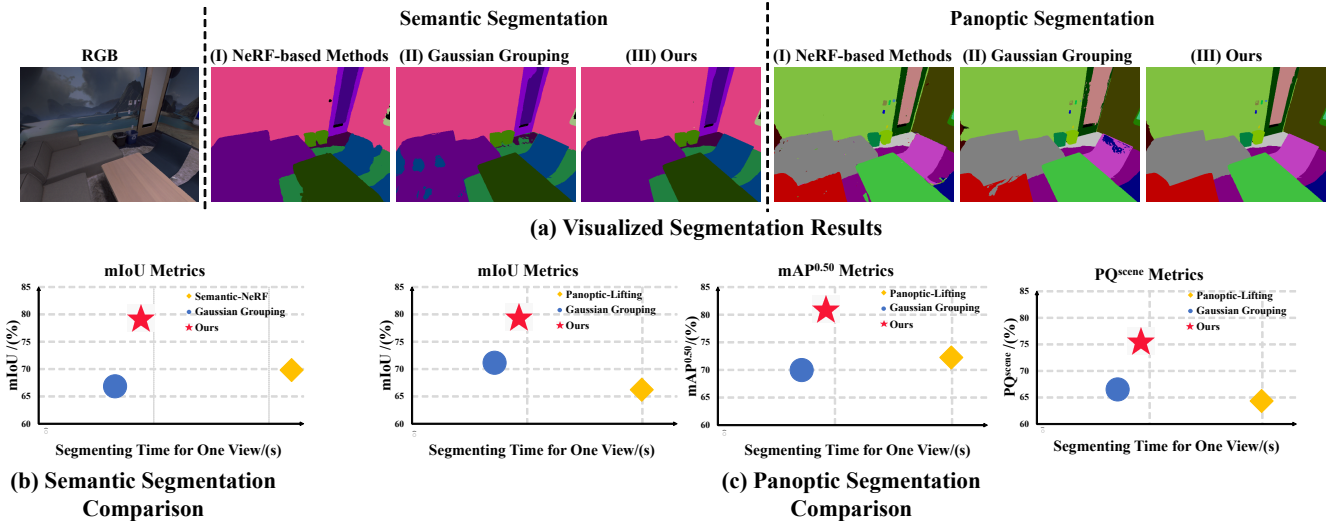


Figure 1: Our method enables compact and swift zero-shot scene segmentation. Compared to Gaussian-based model(Gaussian Grouping), our method achieves significantly more compact zero-shot segmentation, meanwhile delivers rendering speed over 10x faster than NeRF-based segmentation (Semantic-NeRF for semantic and Panoptic-Lifting for panoptic segmentation), as shown qualitatively in (a) and quantitatively in (b) and (c).

Abstract

We propose **Compact and Swift Segmenting 3D Gaussians(CoSSegGaussians)**, a method for compact 3D-consistent scene segmentation at fast rendering speed with only RGB images input. Previous NeRF-based segmentation methods have relied on time-consuming neural scene optimization. While recent 3D Gaussian Splatting has notably improved speed, existing Gaussian-based segmentation methods struggle to produce compact masks, especially in zero-shot segmentation. This issue probably stems from their straightforward assignment of learnable parameters to each Gaussian, resulting in a lack of robustness against cross-view inconsistent 2D machine-generated labels. Our method aims to address this problem by employing Dual Feature Fusion Network as Gaussians' segmentation field. Specifically, we first optimize 3D Gaussians under RGB supervision. After Gaussian Locating, DINO features extracted

from images are applied through explicit unprojection, which are further incorporated with spatial features from the efficient point cloud processing network. Feature aggregation is utilized to fuse them in a global-to-local strategy for compact segmentation features. Experimental results show that our model outperforms baselines on both semantic and panoptic zero-shot segmentation task, meanwhile consumes less than 10% inference time compared to NeRF-based methods. Code and more results will be available at <https://David-Dou.github.io/CoSSegGaussians>

1 Introduction

In recent years, computer vision and computer graphics have achieved notable advancements, particularly in the neural rendering area. Neural Radiance Field(NeRF)[Mildenhall *et al.*, 2021] and its subsequent methods have propelled the development of neural scene representations, which have shown significant capabilities for novel view synthesis.

Besides learning a radiance field, some methods extended from NeRF achieve 3D-consistent segmentation for scene understanding. Early segmenting models have relied on manually annotated 2D masks as supervision and employ time-consuming ray-marching volume rendering. After the release of large vision models like DINO-ViT[Caron *et al.*, 2021] and SAM[Kirillov *et al.*, 2023], NeRF-based methods can achieve few-shot or zero-shot scene segmentation with the introduction of semantically meaningful knowledge or machine-generated labels. Recently, benefiting from the emergence of 3D Gaussian Splatting[Kerbl *et al.*, 2023] which utilizes point-like Gaussians as scene representation and employs rapid rasterization for rendering, some methods have been built on 3D Gaussians for further swift zero-shot segmentation, such as Gaussian Grouping[Ye *et al.*, 2023]. Nevertheless, as illustrated in Fig. 1 (a,II), previous Gaussian-based models struggle to achieve compact segmentation, i.e., providing the same label inside semantic-level or instance-level one object. By assigning learnable parameters for each Gaussian which are updated sensitively according to each viewpoint’s zero-shot mask, they will suffer from segmenting incompactness caused by cross-view inconsistency of the generated 2D labels. Though Gaussian Grouping employs mask association technique for 3D-consistent enhancement and spatial-based regularization for segmenting compactness, inconsistency on some viewpoints still occurs especially for complex scenes and the KNN-based spatial regularization serves as loose constraints which may fail for large-scale objects. Fig. 2 shows that Gaussian Grouping fails to segment some large-scale object areas(*ground* and *cabinet*) reliably due to the inconsistency of zero-shot labels, which will lead to failure for downstream tasks, like scene editing.

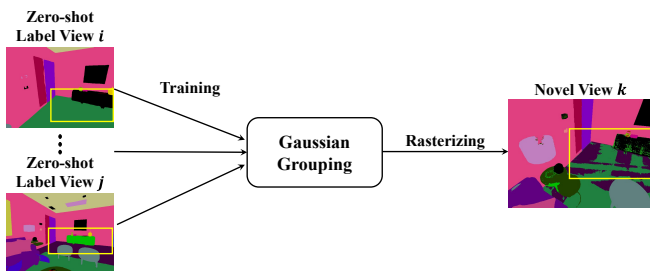


Figure 2: Incompact segmentation caused by cross-view inconsistency in previous Gaussian-based method, such as the selected *ground* and *cabinet* area.

To achieve compact and swift scene segmentation especially for zero-shot situation(see Fig. 1 (a,III)), our goal is to design a compactly segmenting model based on 3D Gaussians. To enhance the segmentation field’s robustness against cross-view inconsistent labels, it’s conjectured that replacing learnable attributes attached on each Gaussian with a decoder upon reasonable priors could be effective. This is because decoding based on strong segmenting priors will be much less sensitive to minor inconsistencies in labels. Motivated by the DINO feature distillation in interactive scene segmentation and spatial information extraction serving as the basis for point cloud segmentation, we believe that fusion of DINO

and spatial features on point-like 3D Gaussians can be used as effective segmenting priors.

Therefore in this paper, we propose CoSSegGaussians, which represents Gaussians’ segmentation field with the proposed Dual Feature Fusion Network. Specifically, our method first optimizes 3D Gaussian scene representation to locate Gaussians. Then considering the explicitness of Gaussians, instead of applying learning-based distillation in [Tschernetzki *et al.*, 2022; Kobayashi *et al.*, 2022; Zhou *et al.*, 2023], we introduce extracted DINO features into 3D Gaussians through explicit unprojection and multi-scale features are used to enhance model’s perceptive ability for scene segmentation. Encoding layers of RandLA-Net[Hu *et al.*, 2020] are employed to extract Gaussians’ spatial features. For further segmentation, the feature aggregation module employs a MLP to decode the fused DINO and spatial features from a global to local perspective, enabling acquisition of compact segmentation logits.

In summary, our work makes the following contributions:

- We propose the Dual Feature Fusion Network to represent 3D Gaussian segmentation field instead of learnable parameters on each Gaussian, which will enhance the segmenting compactness especially in zero-shot segmentation.
- We present an explicit method to introduce extracted 2D DINO features into 3D Gaussians by utilizing unprojection.
- We design a global-to-local feature aggregation module, which fuses multi-scale DINO and spatial features for segmentation.

2 Related Work

2.1 Neural Scene Representation

Neural scene representation has seen significant advancements in recent years. NeRF[Mildenhall *et al.*, 2021] utilizes neural networks to encode 3D scene’s geometry and appearance, combining ray-marching volume rendering to achieve novel view synthesis. Subsequent works have introduced numerous improvements, as NeRF++[Zhang *et al.*, 2020], MipNeRF[Barron *et al.*, 2021], MipNeRF360[Barron *et al.*, 2022] and Tri-MipRF[Hu *et al.*, 2023] aim to enhance rendering quality, while Plenoxel[Fridovich-Keil *et al.*, 2022], DVGO[Sun *et al.*, 2022], TensoRF[Chen *et al.*, 2022] and Instant NGP[Müller *et al.*, 2022] focus on accelerating neural scene optimization. Recently, 3D Gaussian Splatting[Kerbl *et al.*, 2023] has been proposed to represent the scene using 3D Gaussians, which garners widespread attention due to its ability to achieve high-quality and real-time rendering. To improve model’s optimization and inference speed, our model is built on the efficient 3D Gaussian representation.

2.2 Scene Segmentation Methods

For 3D scene understanding, numerous approaches have been developed to extend NeRF to segmentation field, using merely 2D labels as supervision. Semantic-NeRF[Zhi *et al.*, 2021] and DM-NeRF[Wang *et al.*, 2022] facilitate concurrent optimization of the radiance and segmentation field to achieve 3D-consistent scene segmentation which rely on dense-view annotated labels. Benefiting from the development of pre-trained zero-shot 2D segmentation models, some methods

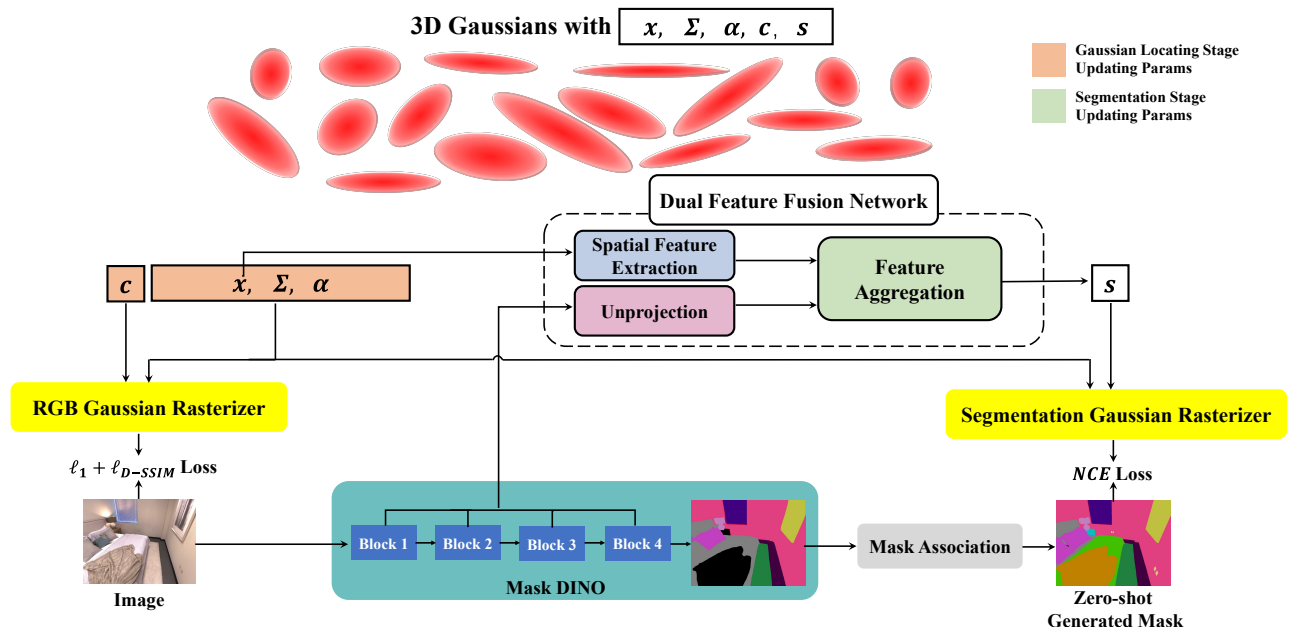


Figure 3: Overview of our method. Our model performs segmentation by capturing 3D Gaussians with geometric, appearance and segmenting features. Gaussians’ geometric information is firstly obtained via differentiable rasterizer, supervised by ℓ_1 and ℓ_{D-SSIM} photometric loss in Gaussian Locating Stage. In further Segmentation Stage, the proposed Dual Feature Fusion, which fuses multi-scale unprojected DINO features and extracted spatial features using a global-to-local feature aggregation module, is applied to generate features s . s is supervised by the zero-shot segmented and associated masks with NCE loss.

have been developed for segmenting scenes without manually labeled annotations. Panoptic Lifting[Siddiqui *et al.*, 2023] is built on TensorRF and aims to achieve zero-shot panoptic segmentation using Mask2Former[Cheng *et al.*, 2022]. Gaussian Grouping[Ye *et al.*, 2023] extends 3D Gaussians by jointly reconstructing and segmenting anything in 3D scenes to achieve rapid scene segmentation. In addition, some interactive segmentation methods are also proposed to segment 3D object in the scene according to user’s prompt on single-view. They often distill large-model extracted 2D knowledge into neural scene representation via rendering to transfer user-provided information. For example, DFF[Kobayashi *et al.*, 2022] and ISRF[Goel *et al.*, 2023] distill knowledge from DINO for click-prompted and language-prompted segmentation, respectively. SAGA[Cen *et al.*, 2023] applies features from SAM[Kirillov *et al.*, 2023] to 3D Gaussian representation for fast and compact interactive segmentation.

For scenes represented with point clouds, segmentation methods have also been presented using points’ spatial information. Considering that 3D Gaussian is a point-like representation, we hypothesize that modules in point cloud segmentation can be extended to Gaussian-based methods. PointNet[Qi *et al.*, 2017a], PointNet++[Qi *et al.*, 2017b], SPG[Landrieu and Simonovsky, 2018] can be used for scene point cloud segmentation, however, they are computationally expensive due to their sampling strategy or graph partitioning. RandLA-Net[Hu *et al.*, 2020] employs rapid random sampling combined with Local Feature Aggregation(Local Spatial Encoding+Attentive Pooling) to improve model efficiency, particularly for large-scale point cloud. Trading-off

the efficiency and performance, we try to introduce spatial information from the swift RandLA-Net to 3D Gaussians.

3 Method

Given only posed RGB images of a 3D scene, our method aims to build an expressive representation to capture geometry, appearance as well as compact segmenting identity of the scene. Our proposed model, CoSSegGaussians, enables compact novel-view 3D-consistent segmentation, while consuming much less rendering time compared to NeRF-based methods. Fig. 3 provides an overview of CoSSegGaussians’ architecture. As the method is based on the recent 3D Gaussian Splatting, we first introduce 3D Gaussian scene representation in 3.1. Subsequently, the Dual Feature Fusion Network for capturing compact segmentation field is presented in 3.2. In addition, training strategy of our model is outlined in 3.3.

3.1 3D Gaussian Scene Representation

3D Gaussian splatting is a recent effective scene representation, which achieves remarkable reconstruction quality and exhibits much higher rendering speed compared to Neural Radiance Field. It represents the scene explicitly with 3D Gaussians which share great amount of similarity with the point cloud, as each Gaussian is parameterized by its centroid $x \in R^3$, 3D covariance Σ (represented with *scale* $\in R^3$ and *rotational quaternion* $\in R^4$ jointly), opacity $\alpha \in R$ and color c as the spherical harmonics(SH) coefficients of three degrees. To supervise these learnable attributes, Gaussian Splatting projects them onto 2D imaging plane to render

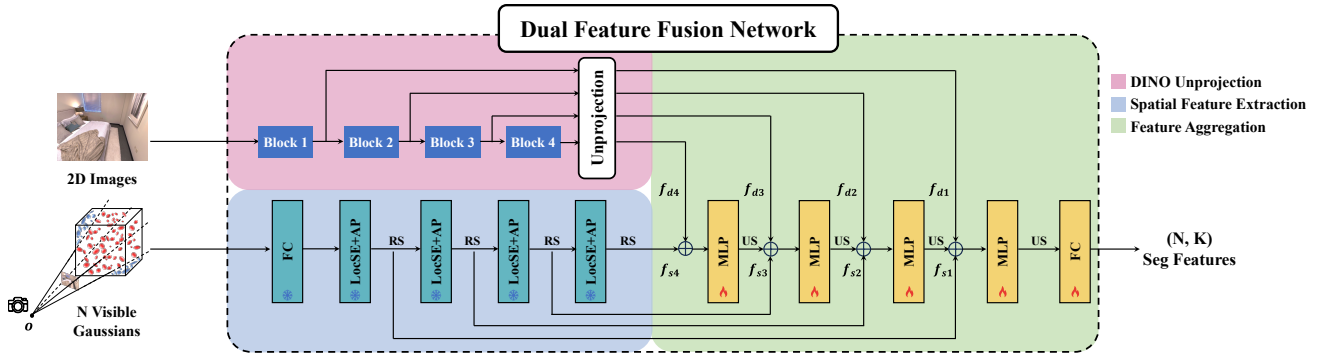


Figure 4: Our proposed Dual Feature Fusion Network. DINO features are introduced into 3D Gaussians through unprojection. Pre-trained RandLA-Net’s encoding layers (consisting of **Local Spatial Encoding & Attentive Pooling**) are utilized to extract spatial features of N visible Gaussians for each viewpoint. Then the multi-scale features are aggregated from global to local for segmenting feature prediction. (**FC**: Fully Connected Layer, **RS**: Random Sampling, **US**: Up Sampling)

RGB image for the given viewpoint by α -blending, which is a differentiable rasterization method and is implemented GPU-friendly. For each pixel \mathbf{p} , it can be formulated as

$$C(\mathbf{p}) = \sum_{i \in \mathcal{N}} c_i \alpha'_i(\mathbf{p}) \prod_{j=1}^{i-1} (1 - \alpha'_j(\mathbf{p})) \quad (1)$$

where c_i represents the i -th Gaussian’s color, $\alpha'_i(\mathbf{p})$ represents the i -th Gaussian’s influence factor on \mathbf{p} which is obtained by multiplying the projected 2D covariance with the learned per-point opacity α_i .

3.2 Dual Feature Fusion Network

To achieve segmentation with 3D Gaussians, in addition to aforementioned scene representational parameters, we also assign segmenting feature s on each Gaussian which is obtained through our Dual Feature Fusion Network, as illustrated in Fig. 4. DINO and spatial features are applied and they further aggregated, from global to local, to generate segmenting logits s .

Multi-scale DINO Feature Unprojection

Given that more comprehensive and extensive knowledge of the scene will enhance segmenting performance, multi-scale DINO features are introduced into scene representation instead of the single-scale in previous interactive segmentation.

Considering that 3D Gaussians utilize point-like scene representation, here we choose to design an explicit method to introduce 2D DINO features into it. Inspired by the semantic tracing in [Chen *et al.*, 2023] which accomplishes inverse rendering of certain object’s multi-view 2D segmentation masks, it’s hypothesized that a similar approach can be extended to unproject DINO features to 3D Gaussians. Consequently, we apply the weighted-sum unprojection approach on all training views’ DINO feature maps to obtain each Gaussian’s feature and the weight is calculated by the affecting Gaussian’s opacity and transmittance. The i -th Gaussian’s DINO feature for scale n can be expressed as:

$$\mathbf{f}_{d_n, i} = \sum_{\mathbf{p}} \alpha'_i(\mathbf{p}) * \prod_{j=1}^{i-1} (1 - \alpha'_j(\mathbf{p})) * \mathbf{f}_{d_n}(\mathbf{p}), n = 1 \dots 4 \quad (2)$$

where $\mathbf{f}_{d_n}(\mathbf{p})$ represents the n -th scale’s DINO feature vector on pixel \mathbf{p} , and the summation performs on all training views’ pixels if the pixel is affected by the i -th Gaussian.

As the inverse rendering method can also record the affected pixel number for each Gaussian, we manually set threshold to prune Gaussian points according to the counter, which will improve efficiency for further feature processing according to our experiments. Visualization of the unprojected DINO features are provided in **Supplementary Material** to show the effectiveness of our feature unprojection.

Spatial Feature Extraction

Aside from DINO features, Gaussians’ spatial information also contains segmenting knowledge. As 3D Gaussians bear a significant resemblance to point cloud, here we employ RandLA-Net [Hu *et al.*, 2020], an efficient method for segmenting large-scale scene point cloud, as Gaussians’ spatial feature extractor.

As further rasterization-based supervision only depends on Gaussians inside the viewing cone and RandLA-Net releases the strict requirement for complete object point cloud due to its attention module (eliminating the need to split scene into blocks containing complete objects), only N visible Gaussians for each view are utilized as input for model efficiency. Then we treat these Gaussians as points and employ pre-trained **Local Feature Aggregation** blocks (consisting of **Local Spatial Encoding and Attentive Pooling**) with **Random Sampling** on N Gaussians’ centroids. The spatial features from local to global ($n = 1$ to 4) for sampled Gaussians are:

$$\mathbf{f}_{s_n} = \mathbf{RS}(\mathbf{LFA}_{n-1}(\dots \mathbf{RS}(\mathbf{LFA}_1(\mathbf{x}))), n = 1 \dots 4 \quad (3)$$

Feature Aggregation

For the following segmentation prediction, the unprojected DINO priors are integrated with the spatial features, through an aggregation process employing a global-to-local strategy.

Specifically, we concatenate each scale’s unprojected DINO features \mathbf{f}_{d_n} with the extracted spatial features \mathbf{f}_{s_n} and decoded features from previous layer, following a global ($n = 4$)-to-local ($n = 1$) approach. In practice, as point sampling is utilized, multi-scale DINO features are unprojected to all located Gaussians and can be further queried with the sampling id in the concatenation.

After feature aggregation, segmenting features are obtained by the decoding layers’ MLP as the (N, K) segmenting features (K represents segmentation classes in the scene) can be expressed as:

$$s = MLP_s([\mathbf{f}_{d_4} \oplus \mathbf{f}_{s_4}] \cdots [\mathbf{f}_{d_1} \oplus \mathbf{f}_{s_1}]) \quad (4)$$

3.3 Training Strategy

As our Dual Feature Fusion for compact segmentation is based on 3D Gaussians’ positions, the training follows a two-stage strategy: Gaussian Locating Stage and Segmentation Stage.

Gaussian Locating Stage is similar to 3D Gaussian Splatting training, as Gaussians’ centroids \mathbf{x} , covariance Σ , opacities α and colors \mathbf{c} are supervised with ℓ_1 and ℓ_{D-SSIM} loss by comparing rendering with the ground-truth RGB image.

$$\ell_{GL} = \lambda_{rgb} \ell_1 + (1 - \lambda_{rgb}) \ell_{D-SSIM} \quad (5)$$

In Segmentation Stage, multi-scale DINO features are unprojected and fused with spatial features, and the MLP decoder in feature aggregation is the only parameters to be updated. After Dual Feature Fusion, the aforementioned Gaussian Rasterizer is extended from RGB to segmentation field, as segmenting logits \mathbf{S} on pixel \mathbf{p} can be acquired by:

$$\mathbf{S}(\mathbf{p}) = \sum_{i \in \mathcal{N}} s_i \alpha'_i(\mathbf{p}) \prod_{j=1}^{i-1} (1 - \alpha'_j(\mathbf{p})) \quad (6)$$

For the supervisory labels, we first employ a DINO-based 2D segmentation method (i.e. MaskDINO [Li *et al.*, 2023]) to generate masks for all RGBs. Adapting from [Ye *et al.*, 2023], multi-view images of a scene are then treated as a video sequence so a well-trained zero-shot tracker [Cheng *et al.*, 2023] is employed to associate the generated masks for cross-view consistency enhancement. The segmentation parameters are optimized with the NCE loss between the rendering with the generated mask, which can be formulated as:

$$\ell_s = - \sum_{\mathbf{p}} \sum_{k \in K} \kappa_r[k] \log(\mathbf{S}(\mathbf{p})[k]) \quad (7)$$

and the objective for Segmentation Stage is:

$$\ell_{Seg} = \lambda_s \ell_s \quad (8)$$

4 Experiments

We evaluate our method on the novel view semantic and panoptic segmentation task, and further demonstrate the potential for scene manipulation as an application of the model. More experimental setups and results can be found in **Supplementary Material**.

4.1 Experimental Setup

Datasets

We show experimental results on scenes from two public indoor datasets: Replica [Straub *et al.*, 2019] and ScanNet [Dai *et al.*, 2017]. Replica is a 3D dataset containing high-fidelity offices and rooms, and each scene consists of RGB images with corresponding 2D segmentation masks rendered by the

authors of [Zhi *et al.*, 2021]. ScanNet is a challenging real-world dataset with each scene comprising images accompanied by 2D segmenting masks and camera poses. For both datasets, 7 scenes are selected for training and evaluation (similar to [Wang *et al.*, 2022]). To generate training labels, we utilize MaskDINO [Li *et al.*, 2023] which is pre-trained on ADE20K [Zhou *et al.*, 2019] followed by DEVA tracker [Cheng *et al.*, 2023] for zero-shot segmentation masks on indoor scene images. The evaluation is conducted between all poses’ segmentation predictions and corresponding targets in the testset. It should be noticed that the annotated segmentation masks are only available in evaluation as targets and are unavailable to the model during training.

Evaluation Metrics

For semantic segmentation performance, we employ the mean intersection over union (**mIoU**) to evaluate the quality of predicted segmentation maps. For panoptic segmentation, aside from **mIoU**, mean average precision (**mAP**) on masks is utilized, with IoU thresholds set at 0.50. In addition, for better evaluation of panoptic segmentation, scene-level panoptic quality (**PQ^{scene}**) derived from [Siddiqui *et al.*, 2023] is introduced for every scene, as we compare all pairs of *thing* or *stuff* segmentation subsets for all renderings in each scene instead of one rendered image, and record a match when $\text{IoU} > 0.50$.

In addition to the above performance metrics, **FPS** (Frames Per Second) and learnable parameters in training are also used to evaluate model efficiency.

Multi-scale Features Setup

In reference to feature distillation works [Tschernetzki *et al.*, 2022; Kobayashi *et al.*, 2022], DINO-ViT is used as teacher network to extract semantically meaningful prior from RGB images. For multi-scale setting, we select outputs of 4 transformer blocks inspired by [Sharma *et al.*, 2023]. Before unprojection to 3D Gaussians, these features are concatenated with the expanded global feature tensor then reduced to 64 dimensions by PCA and L_2 normalized.

For spatial features, RandLA-Net pre-trained on the large-scale indoor dataset S3DIS [Armeni *et al.*, 2017] is employed, with its encoding layers frozen during training.

Implementation Details

Our method is implemented based on Gaussian Splatting [Kerbl *et al.*, 2023] and RandLA-Net [Hu *et al.*, 2020] (PyTorch implementation). We add segmentation logits, which is the processed result from our Dual Feature Fusion Network, as a feature on each Gaussian and implement forward & backward rasterization in reference to [Ye *et al.*, 2023]. In training, $\lambda_{rgb} = 0.8$ and $\lambda_s = 0.1$. Adam optimizer is used for updating both Gaussian parameters and the feature aggregation network, with the former’s learning rates identical to Gaussian Splatting and 0.001 for MLP network. All datasets are trained for 10K iterations on one NVIDIA A800 GPU.

4.2 Comparisons

We conduct a comparative analysis on two kinds of segmentation tasks: semantic and panoptic segmentation, as the former assigns semantic labels for all pixels, and the latter [Kirillov *et al.*, 2019] attaches labels for both foreground

objects(defined as *thing*) and background(defined as *stuff*) while provides object-level labels only for *thing*. In training, MaskDINO’s semantic and panoptic modes are employed to generate zero-shot 2D segmentation labels for each task respectively, which are further associated by pre-trained video tracker. We compare our method with NeRF-based 3D segmentation methods(Semantic-NeRF[Zhi *et al.*, 2021] in semantic segmentation and Panoptic-Lifting[Siddiqui *et al.*, 2023], a segmenting method built on TensorRF for acceleration, in panoptic segmentation) and the recent Gaussian-based segmentation, i.e. Gaussian Grouping[Ye *et al.*, 2023], which are all trained with the same generated labels and evaluated on all test viewpoints. All statistics reported further are the average numbers across all scene metrics in each dataset.

Semantic Segmentation

Model	Replica			ScanNet		
	mIoU(%)	FPS	Learnable Params(MB)	mIoU(%)	FPS	Learnable Params(MB)
Semantic-NeRF	69.81	≈ 5	9.7	69.67	≈ 5	10.4
Gaussian Grouping	66.84	≈140	838.0	67.99	≈150	838.6
Ours	79.34	≈ 90	680.3	75.40	≈100	684.5

Table 1: Comparison on zero-shot novel-view semantic segmentation. Our model outperforms both baselines and achieves much faster speed compared to the Semantic-NeRF, showcasing our efficient tackling for compact and swift zero-shot scene segmentation.

Tab. 1 shows segmentation results under zero-shot 2D semantic label supervision. It can be observed that our method obtains remarkably higher segmenting performance (+9.53%/5.73% mIoU on Replica/ScanNet than Semantic-NeRF, +12.50%/7.41% mIoU than Gaussian Grouping). Though sacrificing some speed compared to Gaussian Grouping, our method still achieves a significantly faster speed than the NeRF-based model(approximately 20x). The performance improvement from Gaussian Grouping justifies the slightly increased time consumption.

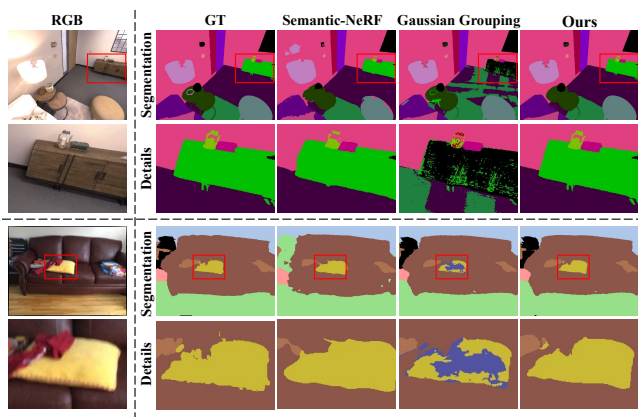


Figure 5: Qualitative comparison on semantic segmentation.

Similar performance improvement can also be observed qualitatively in Fig. 5. We find that Gaussian Grouping fail to provide compact semantic masks especially for some

large-scale objects such as *ground*, *cabinet*(above) and *pillow*(below). The limitation may stem from the lack of grouping constraints for large objects as Gaussian Grouping’s 3D regularization loss only restricts K spatial neighbors’ features. In contrast, our method, which incorporates DINO and spatial features, can enhance the segmenting compactness of these objects and consequently improve performance.

Panoptic Segmentation

Quantitative panoptic segmentation results are presented in Tab. 2, which also showcase that our model can outperform baselines, leading to approximately 10%/9%/10% improvement in $mIoU/mAP^{0.50}/PQ^{scene}$ compared to Panoptic-Lifting and 7%/10%/8% improvement in $mIoU/mAP^{0.50}/PQ^{scene}$ compared to Gaussian Grouping. It can be noticed that Gaussian Grouping achieves better panoptic than semantic segmentation, mainly due to its KNN grouping for segmenting scenes finer-grainedly. However, our method still surpasses it by fusing dual features with a slightly longer time, which serves as a more tight and compact spatial regularization way.

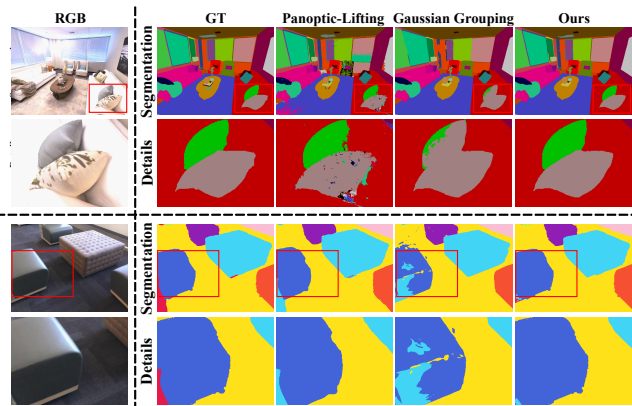


Figure 6: Qualitative comparison on panoptic segmentation.

As depicted in Fig 6, Panoptic-Lifting and Gaussian Grouping fail to segment some objects compactly such as the *pillow*(above) and *seat*(below). Conversely, our model alleviates the problem and provides a more compact segmentation.

4.3 Ablation Studies

To discover each component’s contribution to zero-shot segmenting improvement, a series of ablation experiments on semantic segmentation task are conducted for the Replica dataset using the same generated training labels. As a first baseline (Tab 3 row 1), we disable both unprojected DINO and spatial features, and train the segmenting features on Gaussians from scratch. Though achieving faster speed, the baseline will suffer from a significant performance decrease(-17.55% mIoU) compared to the full model. Visualized segmentation results and segmented 3D Gaussians in Fig 7 (a) also demonstrate the performance decline.

DINO Feature Unprojection

To verify the effect of applying DINO feature through unprojection, we conduct a comparison between the model without DINO unprojection(using only spatial information to pre-

Model	Replica					ScanNet				
	mIoU(%)	mAP ^{0.50} (%)	PQ ^{scene} (%)	FPS	Learnable Params(MB)	mIoU(%)	mAP ^{0.50} (%)	PQ ^{scene} (%)	FPS	Learnable Params(MB)
Panoptic-Lifting	66.22	72.25	64.34	≈ 10	100.1	67.01	66.95	60.74	≈ 10	102.5
Gaussian Grouping	71.15	69.98	66.52	≈140	840.2	68.70	67.03	61.83	≈150	841.6
Ours	79.49	80.97	75.60	≈ 90	681.1	74.37	76.14	68.68	≈ 90	685.4

Table 2: Comparison on zero-shot novel-view panoptic segmentation. Our model’s performance advantage similar to semantic segmentation also occurs in the task.

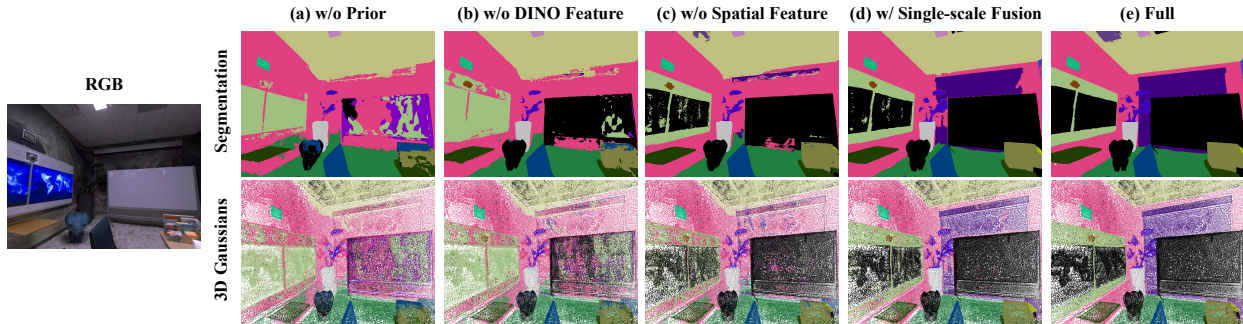


Figure 7: Visualized ablation results. Rendered segmentation maps along with segmented 3D Gaussians are presented.

Spatial Feature	DINO Feature	mIoU(%)	FPS
×	×	61.79	≈160
✓	×	67.53	≈110
×	✓	72.33	≈150
✓	✓ (single-scale fusion)	75.69	≈100
✓	✓	79.34	≈ 90

Table 3: Ablation results on segmenting performance and speed.

dict segmentation logits) with the full model. A comparison between Tab. 3 row 2 and row 5 reveals that the addition of DINO unprojection leads to remarkable improvement in segmentation (mIoU +11.81%). As depicted in Fig 7 (b) and (e), the full model exhibits inferior performance as the unprojected semantically meaningful correspondences can enhance segmenting compactness for large objects, like the *board*. These findings clearly indicate the essential role of DINO features in zero-shot segmentation.

Gaussians Spatial Features’ Utilization

The impact of Gaussian points’ spatial features is also evaluated, as we set the spatial features extracted from RandLANet unavailable as ablation. As shown in Tab. 3 row 3, the absence of spatial information results in a performance decline(-7.01% mIoU) which can also be demonstrated by Fig. 7 (c).

Furthermore, FPS comparison on Tab. 3 row 1, row 3 and row 5 indicates that extracting and processing Gaussian’s spatial features cause the time consumption, leading to a 60 FPS decrease approximately. However, such time cost is not overly burdensome in practice due to the swift Gaussian rendering, and the enhancement for segmenting performance underscores its importance.

Multi-scale Feature Aggregation

Additionally, we assess the effect of our designed multi-scale(global-to-local) DINO and spatial feature aggregation module by conducting the single-scale fusion experiment. As shown in Tab. 3 row 5, the absence of multi-scale feature aggregation results in a performance decrease, a 3.65% mIoU decline. By comparing Fig. 7 (e) with (d), we find multi-scale fusion can further enhance the segmenting compactness for objects, such as the *screen*.

4.4 Application

Once our model is trained under panoptic segmentation mode, in addition to generating novel-view segmentation masks, it can also be used for further 3D object-level applications, such as scene manipulation, i.e., novel-view synthesis with 3D object removed, duplicated or manipulated under affine transformations. Benefiting from the explicitness of 3D Gaussians representation, we can conveniently apply manipulations on the trained scene.

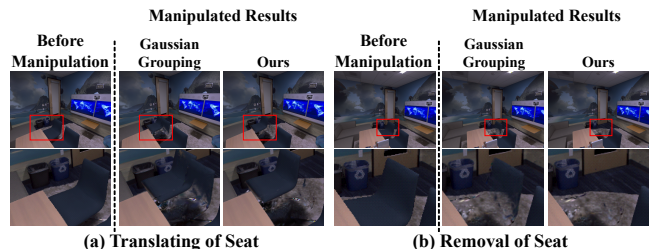


Figure 8: Scene manipulation results Compared to Gaussian Grouping[Ye *et al.*, 2023], our model can get higher fidelity results.

Fig. 8 shows that our method can achieve more realistic results for scene manipulation, compared to Gaussian Group-

ing, due to the segmenting compactness improvement. More applications such as the language-based 3D object segmentation (based on 2D language-based segmentation model such as Text2Seg[Zhang *et al.*, 2023] and Grounding DINO[Liu *et al.*, 2023]) are available in **Supplementary Material**.

4.5 Limitations and Future Work

Though our model utilizes fewer learnable parameters compared to previous Gaussian-based method as reported in Tab. 1 and Tab. 2, the GPU occupancy reaches a high level during training for storing computation graphs of the MLP on Gaussian points. This is the case even though our spatial feature extraction are designed to process only the visible inside the viewing cone instead of the whole scene’s Gaussians, the point number still reaches 10^5 order of magnitude.

Therefore in the future, we intend to make efforts to reduce GPU occupancy, for example, by reconstructing 3D Gaussians from sparser point cloud initialization. In addition, we plan to add structural constraint loss, such as spatial regularization based on our multi-scale fused features, which may further improve segmenting compactness.

5 Conclusion

We propose CoSSegGaussians, which achieves compact and swift scene segmentation with only posed RGB images. Our method is built on 3D Gaussians and utilizes Dual Feature Fusion Network as segmentation field, which aggregates DINO and spatial features for segmentation. Multi-scale DINO features from images are introduced into located 3D Gaussians via unprojection and are further combined with Gaussians’ spatial information from RandLA-Net. A global-to-local aggregation module is then applied to generate compact segmenting logits. Results illustrate that our model can accomplish the zero-shot segmentation task reliably and efficiently.

References

- Iro Armeni, Sasha Sax, Amir R Zamir, and Silvio Savarese. Joint 2d-3d-semantic data for indoor scene understanding. *arXiv preprint arXiv:1702.01105*, 2017.
- Jonathan T Barron, Ben Mildenhall, Matthew Tancik, Peter Hedman, Ricardo Martin-Brualla, and Pratul P Srinivasan. Mip-nerf: A multiscale representation for anti-aliasing neural radiance fields. In *Proceedings of the IEEE/CVF International Conference on Computer Vision*, pages 5855–5864, 2021.
- Jonathan T Barron, Ben Mildenhall, Dor Verbin, Pratul P Srinivasan, and Peter Hedman. Mip-nerf 360: Unbounded anti-aliased neural radiance fields. In *Proceedings of the IEEE/CVF Conference on Computer Vision and Pattern Recognition*, pages 5470–5479, 2022.
- Mathilde Caron, Hugo Touvron, Ishan Misra, Hervé Jégou, Julien Mairal, Piotr Bojanowski, and Armand Joulin. Emerging properties in self-supervised vision transformers. In *Proceedings of the IEEE/CVF international conference on computer vision*, pages 9650–9660, 2021.
- Jiazhong Cen, Jiemin Fang, Chen Yang, Lingxi Xie, Xiaopeng Zhang, Wei Shen, and Qi Tian. Segment any 3d gaussians. *arXiv preprint arXiv:2312.00860*, 2023.
- Anpei Chen, Zexiang Xu, Andreas Geiger, Jingyi Yu, and Hao Su. Tensorf: Tensorial radiance fields. In *European Conference on Computer Vision*, pages 333–350. Springer Nature Switzerland Cham, 2022.
- Yiwen Chen, Zilong Chen, Chi Zhang, Feng Wang, Xiaofeng Yang, Yikai Wang, Zhongang Cai, Lei Yang, Huaping Liu, and Guosheng Lin. Gaussianeditor: Swift and controllable 3d editing with gaussian splatting. *arXiv preprint arXiv:2311.14521*, 2023.
- Bowen Cheng, Ishan Misra, Alexander G Schwing, Alexander Kirillov, and Rohit Girdhar. Masked-attention mask transformer for universal image segmentation. In *Proceedings of the IEEE/CVF conference on computer vision and pattern recognition*, pages 1290–1299, 2022.
- Ho Kei Cheng, Seoung Wug Oh, Brian Price, Alexander Schwing, and Joon-Young Lee. Tracking anything with decoupled video segmentation. In *Proceedings of the IEEE/CVF International Conference on Computer Vision*, pages 1316–1326, 2023.
- Angela Dai, Angel X Chang, Manolis Savva, Maciej Halber, Thomas Funkhouser, and Matthias Nießner. Scannet: Richly-annotated 3d reconstructions of indoor scenes. In *Proceedings of the IEEE conference on computer vision and pattern recognition*, pages 5828–5839, 2017.
- Sara Fridovich-Keil, Alex Yu, Matthew Tancik, Qinhong Chen, Benjamin Recht, and Angjoo Kanazawa. Plenoxels: Radiance fields without neural networks. In *Proceedings of the IEEE/CVF Conference on Computer Vision and Pattern Recognition*, pages 5501–5510, 2022.
- Rahul Goel, Dhawal Sirikonda, Saurabh Saini, and PJ Narayanan. Interactive segmentation of radiance fields. In *Proceedings of the IEEE/CVF Conference on Computer Vision and Pattern Recognition*, pages 4201–4211, 2023.
- Qingyong Hu, Bo Yang, Linhai Xie, Stefano Rosa, Yulan Guo, Zhihua Wang, Niki Trigoni, and Andrew Markham. Randla-net: Efficient semantic segmentation of large-scale point clouds. In *Proceedings of the IEEE/CVF conference on computer vision and pattern recognition*, pages 11108–11117, 2020.
- Wenbo Hu, Yuling Wang, Lin Ma, Bangbang Yang, Lin Gao, Xiao Liu, and Yuewen Ma. Tri-miprf: Tri-mip representation for efficient anti-aliasing neural radiance fields. In *Proceedings of the IEEE/CVF International Conference on Computer Vision*, pages 19774–19783, 2023.
- Bernhard Kerbl, Georgios Kopanas, Thomas Leimkühler, and George Drettakis. 3d gaussian splatting for real-time radiance field rendering. *ACM Transactions on Graphics*, 42(4), 2023.
- Alexander Kirillov, Kaiming He, Ross Girshick, Carsten Rother, and Piotr Dollár. Panoptic segmentation. In *Proceedings of the IEEE/CVF conference on computer vision and pattern recognition*, pages 9404–9413, 2019.

- Alexander Kirillov, Eric Mintun, Nikhila Ravi, Hanzi Mao, Chloe Rolland, Laura Gustafson, Tete Xiao, Spencer Whitehead, Alexander C Berg, Wan-Yen Lo, et al. Segment anything. *arXiv preprint arXiv:2304.02643*, 2023.
- Sosuke Kobayashi, Eiichi Matsumoto, and Vincent Sitzmann. Decomposing nerf for editing via feature field distillation. *Advances in Neural Information Processing Systems*, 35:23311–23330, 2022.
- Loic Landrieu and Martin Simonovsky. Large-scale point cloud semantic segmentation with superpoint graphs. In *Proceedings of the IEEE conference on computer vision and pattern recognition*, pages 4558–4567, 2018.
- Feng Li, Hao Zhang, Huaizhe Xu, Shilong Liu, Lei Zhang, Lionel M Ni, and Heung-Yeung Shum. Mask dino: Towards a unified transformer-based framework for object detection and segmentation. In *Proceedings of the IEEE/CVF Conference on Computer Vision and Pattern Recognition*, pages 3041–3050, 2023.
- Shilong Liu, Zhaoyang Zeng, Tianhe Ren, Feng Li, Hao Zhang, Jie Yang, Chunyuan Li, Jianwei Yang, Hang Su, Jun Zhu, et al. Grounding dino: Marrying dino with grounded pre-training for open-set object detection. *arXiv preprint arXiv:2303.05499*, 2023.
- Ben Mildenhall, Pratul P Srinivasan, Matthew Tancik, Jonathan T Barron, Ravi Ramamoorthi, and Ren Ng. Nerf: Representing scenes as neural radiance fields for view synthesis. *Communications of the ACM*, 65(1):99–106, 2021.
- Thomas Müller, Alex Evans, Christoph Schied, and Alexander Keller. Instant neural graphics primitives with a multiresolution hash encoding. *ACM Transactions on Graphics (TOG)*, 41(4):1–15, 2022.
- Charles R Qi, Hao Su, Kaichun Mo, and Leonidas J Guibas. Pointnet: Deep learning on point sets for 3d classification and segmentation. In *Proceedings of the IEEE conference on computer vision and pattern recognition*, pages 652–660, 2017.
- Charles Ruizhongtai Qi, Li Yi, Hao Su, and Leonidas J Guibas. Pointnet++: Deep hierarchical feature learning on point sets in a metric space. *Advances in neural information processing systems*, 30, 2017.
- Prafull Sharma, Julien Philip, Michaël Gharbi, Bill Freeman, Fredo Durand, and Valentin Deschaintre. Materialistic: Selecting similar materials in images. *ACM Transactions on Graphics (TOG)*, 42(4):1–14, 2023.
- Yawar Siddiqui, Lorenzo Porzi, Samuel Rota Bulò, Norman Müller, Matthias Nießner, Angela Dai, and Peter Kotschieder. Panoptic lifting for 3d scene understanding with neural fields. In *Proceedings of the IEEE/CVF Conference on Computer Vision and Pattern Recognition*, pages 9043–9052, 2023.
- Julian Straub, Thomas Whelan, Lingni Ma, Yufan Chen, Erik Wijmans, Simon Green, Jakob J Engel, Raul Mur-Artal, Carl Ren, Shobhit Verma, et al. The replica dataset: A digital replica of indoor spaces. *arXiv preprint arXiv:1906.05797*, 2019.
- Cheng Sun, Min Sun, and Hwann-Tzong Chen. Direct voxel grid optimization: Super-fast convergence for radiance fields reconstruction. In *Proceedings of the IEEE/CVF Conference on Computer Vision and Pattern Recognition*, pages 5459–5469, 2022.
- Vadim Tschernezki, Iro Laina, Diane Larlus, and Andrea Vedaldi. Neural feature fusion fields: 3d distillation of self-supervised 2d image representations. In *2022 International Conference on 3D Vision (3DV)*, pages 443–453. IEEE, 2022.
- Bing Wang, Lu Chen, and Bo Yang. Dm-nerf: 3d scene geometry decomposition and manipulation from 2d images. *arXiv preprint arXiv:2208.07227*, 2022.
- Mingqiao Ye, Martin Danelljan, Fisher Yu, and Lei Ke. Gaussian grouping: Segment and edit anything in 3d scenes. *arXiv preprint arXiv:2312.00732*, 2023.
- Kai Zhang, Gernot Riegler, Noah Snavely, and Vladlen Koltun. Nerf++: Analyzing and improving neural radiance fields. *arXiv preprint arXiv:2010.07492*, 2020.
- Jielu Zhang, Zhongliang Zhou, Gengchen Mai, Lan Mu, Mengxuan Hu, and Sheng Li. Text2seg: Remote sensing image semantic segmentation via text-guided visual foundation models. *arXiv preprint arXiv:2304.10597*, 2023.
- Shuaifeng Zhi, Tristan Laidlow, Stefan Leutenegger, and Andrew J Davison. In-place scene labelling and understanding with implicit scene representation. In *Proceedings of the IEEE/CVF International Conference on Computer Vision*, pages 15838–15847, 2021.
- Bolei Zhou, Hang Zhao, Xavier Puig, Tete Xiao, Sanja Fidler, Adela Barriuso, and Antonio Torralba. Semantic understanding of scenes through the ade20k dataset. *International Journal of Computer Vision*, 127(3):302–321, 2019.
- Shijie Zhou, Haoran Chang, Sicheng Jiang, Zhiwen Fan, Zehao Zhu, Dejia Xu, Pradyumna Chari, Suyu You, Zhangyang Wang, and Achuta Kadambi. Feature 3dgs: Supercharging 3d gaussian splatting to enable distilled feature fields. *arXiv preprint arXiv:2312.03203*, 2023.